



Project Casper  
Flight Readiness Review  
(FRR) Addendum  
Purdue University 2020

**500 Allison Road**  
**West Lafayette, IN 47906**  
Purdue Space Program

# Table of Contents

<b>Summary of FRR Addendum</b>	<b>4</b>
Team Summary	4
PSP-SL 2020 Executive Board	4
Purpose of Flights	4
Flight Summary Information	4
VDF/PDF #1	5
VDF/PDF #2	6
Changes Made Since First VDF/PDF	8
Changes Made to the Vehicle Design	8
Changes Made to the Payload Design	9
<b>Results of Vehicle Demonstration Re-Flight</b>	<b>10</b>
Summary of Vehicle Demonstration Flights	10
Re-Flight Systems With Proper Functionality	10
Re-Flight Systems Without Proper Functionality	10
Flight Profile	11
Updated Simulations	11
Hardware Rebuilt Since VDF 1	15
Lessons Learned Concerning the Vehicle	16
<b>Vehicle</b>	<b>16</b>
<b>Results of Payload Demonstration Flights</b>	<b>17</b>
Payload R&D System Design	17
R&D Design Summary	17
UAV Retention System	17
Locking System	17
Axial Expansion System	18
UAV Orientation Control System	19
R&D Re-Flight Systems with Proper Functionality	20
R&D Re-Flight Systems Without Proper Functionality	21
R&D Hardware Rebuilt Since PDF 1	21
Lessons Learned Concerning R&D	21
Payload Mission	22
Payload Mission Design Summary	22
<b>Table 3.2: Payload Demonstration Flight Contingencies</b>	<b>24</b>

---

Payload Re-Flight Systems With Proper Functionality	24
Payload Re-Flight Systems Without Proper Functionality	25
Payload Hardware Rebuilt Since PDF 1	26
Lessons Learned Concerning the Payload	26
<b>Changes Made to Team Safety since VDF/PDF #1</b>	<b>27</b>
Checklist Improvements	27
Quality Witness Improvements	27
<b>Official Altimeter Data</b>	<b>28</b>
Initial Flight (VDF/PDF 1) on 2/15/2019	28
Re-Flight (VDF/PDF 2) on 3/7/2019	28

## 1. Summary of FRR Addendum

The following sections summarize information about the 2020 Purdue Space Program Student Launch (PSP-SL) team, its mentor, its vehicle demonstration flights (VDFs) and payload demonstration flights (PDFs), and the changes made to its vehicle and payload since the PSP-SL FRR report.

### 1.1. Team Summary

<b>Team Name</b>	PSP-SL (Purdue Space Program - Student Launch)
<b>Mailing Address</b>	2604 Bristlecone Dr., West Lafayette, IN 47906
<b>2020 Team Mentor</b>	Victor Barlow
<b>2020 Mentor Contact Information</b>	vmbarlow@purdue.edu   (765) 414-2848 (Cell)
<b>2020 Mentor TRA / NAR Certifications</b>	NAR 88988, TRA 6839 TAP, Level 3 Certified

Table 1.1: PSP-SL Team Summary

### 1.2. PSP-SL 2020 Executive Board

Position	Name	Email
<b>Project Manager</b>	Luke Perrin	lperrin@purdue.edu
<b>Assistant Project Manager</b>	Michael Repella	mrepella@purdue.edu
<b>Safety Team Lead</b>	Noah Stover	nstover@purdue.edu
<b>Payload Co-Team Lead</b>	Josh Binion	binionj@purdue.edu
<b>Payload Co-Team Lead</b>	Hicham Belhseine	hbelhsei@purdue.edu
<b>Avionics &amp; Recovery Team Lead</b>	Katelin Zichittella	kzichitt@purdue.edu
<b>Business Team Lead</b>	Natalie Keefer	keefern@purdue.edu
<b>Social &amp; Outreach Team Lead</b>	Skyler Harlow	sharlow@purdue.edu
<b>Construction Team Lead</b>	Lauren Smith	smit3204@purdue.edu
<b>Construction Team Mentor</b>	Zach Carroll	carrollz@purdue.edu

Table 1.2: PSP-SL Executive Board

### 1.3. Purpose of Flights

Two demonstration flights, one on February 15th, 2020, and one on March 7, 2020, were flown with the launch vehicle and payload fully prepared to fly. As such, both flights were meant to act as both vehicle demonstration flights and payload demonstration flights. The first flight acted as the first attempt at both a VDF and a PDF, and the second flight was a vehicle demonstration re-flight and a payload demonstration re-flight.

### 1.4. Flight Summary Information

Listed below is a summary of each test flight. Both times that the team has launched our full-scale vehicle, the payload has been in its final design configuration. Section 1.4.1 discusses the

demonstration flight which occurred on February 15th, 2020 (VDF/PDF #1), and Section 1.4.2 discusses the demonstration flight which occurred on March 7th, 2020 (VDF/PDF #2). Specific information about each of the flights is below.

### 1.4.1.

### VDF/PDF #1

<b>Date of Flight</b>	02/15/2020
<b>Location of Flight</b>	North of Pence, Indiana
<b>Launch Conditions</b>	<b>Temperature:</b> 36F <b>Winds:</b> 14mph SSW <b>Humidity:</b> 68% <b>Overcast</b> <b>Cloud Ceiling:</b> 6000 ft (15 min. before launch - METAR KDNV) 4000 ft (at launch)
<b>Motor Flown</b>	CTI 75mm L1115-0 4 Grain
<b>Ballast Flown</b>	2.5lbm
<b>Final Payload Flown?</b>	Yes
<b>Air Brake System Flown?</b>	No
<b>Official Target Altitude</b>	4325'
<b>Predicted Simulation Altitude</b>	4584'
<b>Measured Altitude</b>	4488' - primary 4688' - secondary 4588' - average
<b>Off-Nominal Events Present?</b>	Yes (See comment)

Table 1.3: VDF/PDF #1 Summary

### Primary Altimeter (Telemetry)

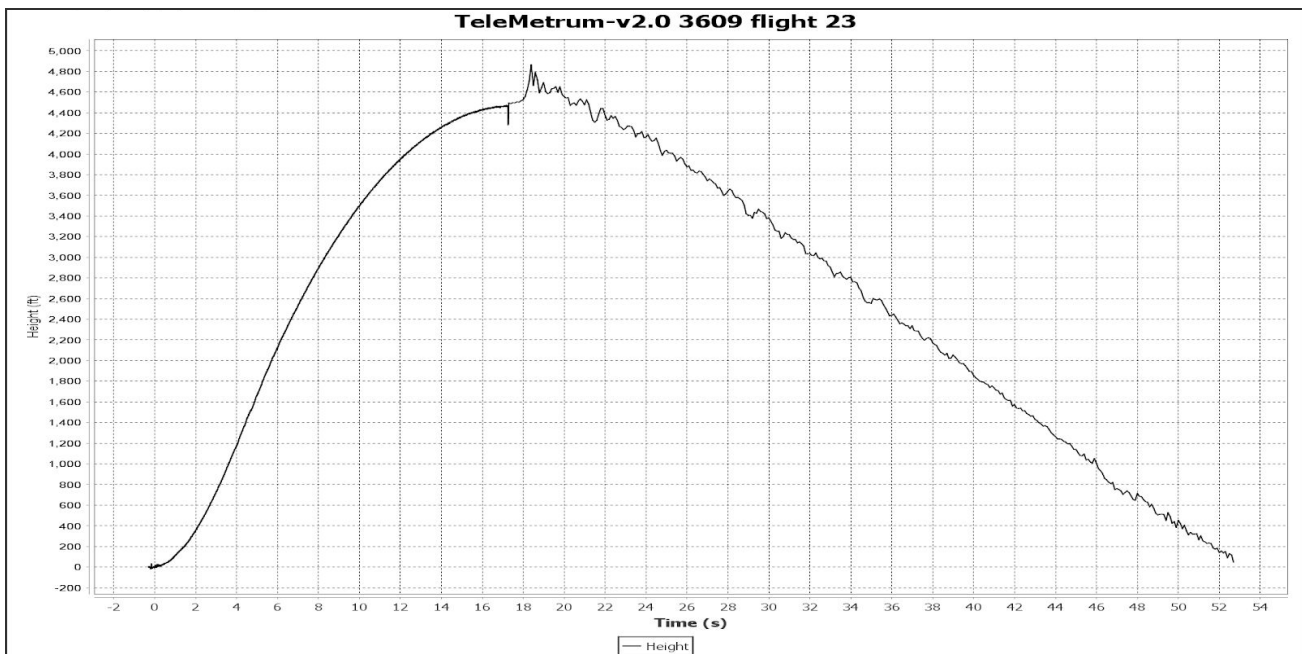


Figure 1.1: Telemetry Altimeter (Primary) Flight Profile

Redundant Altimeter (RRC3+ Sport)

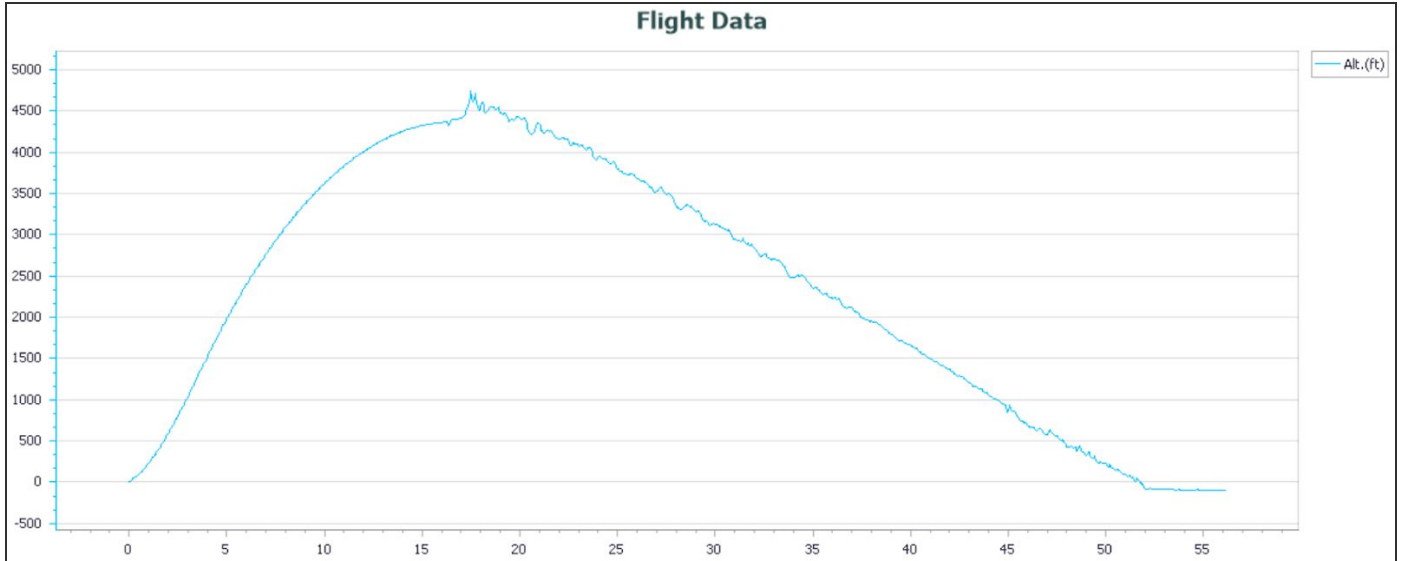


Figure 1.2: RRC3+ Sport Altimeter (Redundant) Flight Profile

1.4.2. VDF/PDF #2

Date of Flight	03/07/2020
Location of Flight	North of Pence, Indiana
Launch Conditions	<b>Temperature:</b> 47F <b>Winds:</b> 9mph S <b>Humidity:</b> 45% <b>Clear Skies</b> <b>Cloud Ceiling:</b> None
Motor Flown	CTI 75mm L1115-0 4 Grain
Ballast Flown	3.75lbm
Final Payload Flown?	Yes
Air Brake System Flown?	No
Official Target Altitude	4325'
Predicted Simulation Altitude	4665'
Measured Altitude	4601' - primary 4625' - secondary 4613' - average
Off-Nominal Events Present?	No

Table 1.4: VDF/PDF #1 Summary

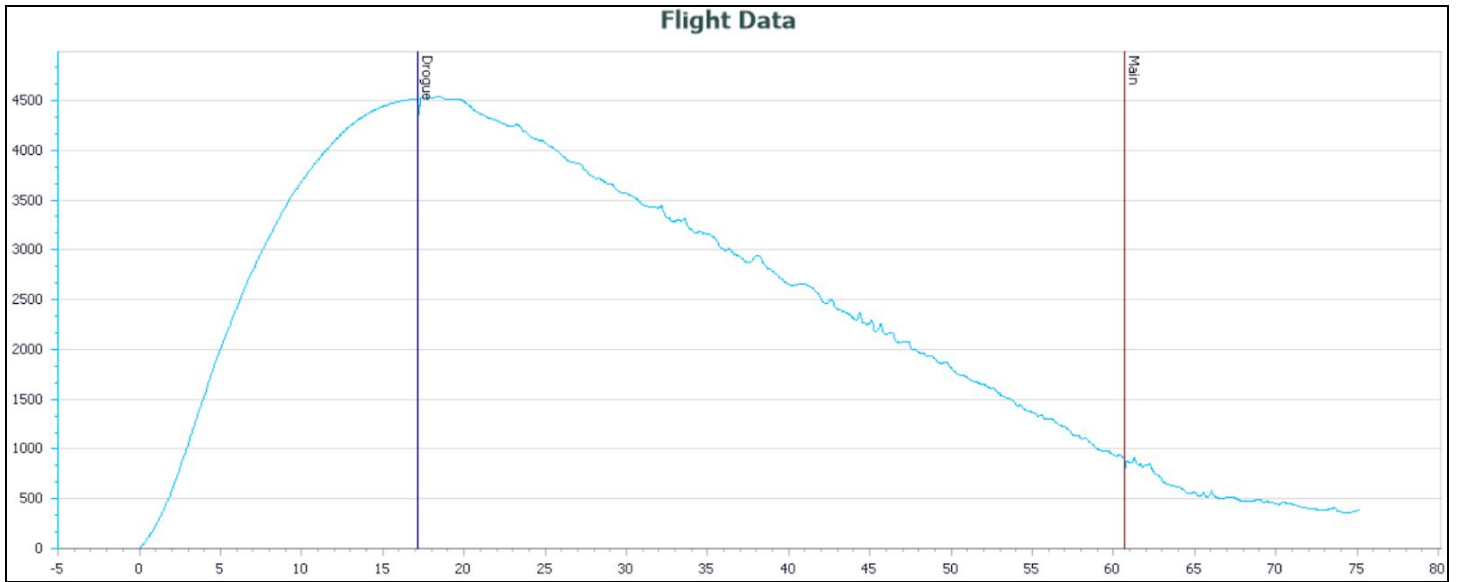


Figure 1.3: RRC3+ Sport Altimeter (Primary) VDF/PDF #2 Flight Profile

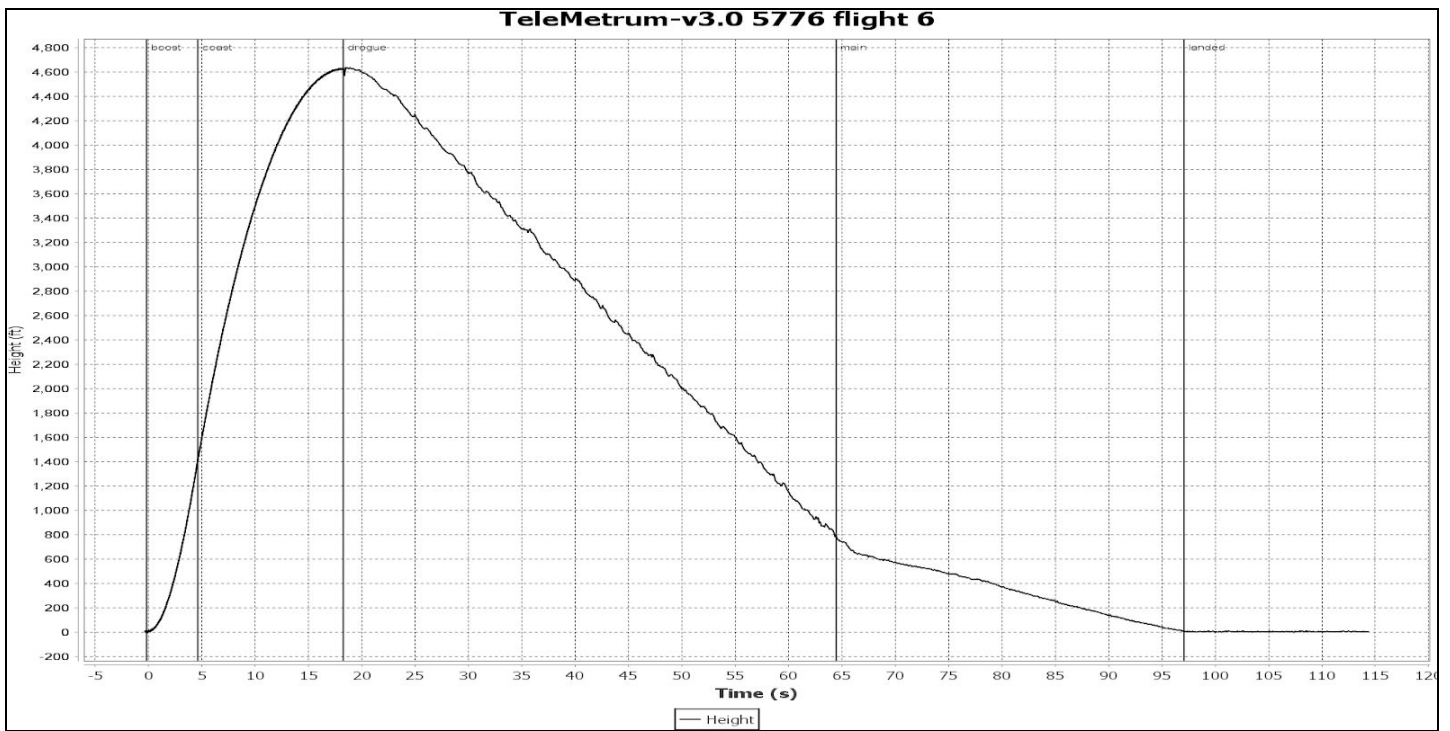


Figure 1.4: Telemetrum Altimeter (Redundant) VDF/PDF #2 Flight Profile

## 1.5. Changes Made Since First VDF/PDF

This section describes how the design of the vehicle and payload design has evolved between the teams first full-scale VDF/PDF and the second VDF/PDF.

### 1.5.1. Changes Made to the Vehicle Design

#### Vehicle

The significant change made to the vehicle design was the reconfiguration of ballast to center the vehicle's weight along its axis of symmetry. This was done by adding custom-machined ballast to the vehicle at the aft end of the payload retention and deployment (R&D) system. This was discussed in both the FRR report and FRR presentation further.

#### Avionics and Recovery

Two significant changes have been made to avionics and recovery since FRR submission. One is that the main parachute deployment altitudes have been updated from 800' above ground level (AGL) for the primary altimeter and 700' AGL for the redundant altimeter to 1000' AGL for the primary altimeter and 800' AGL for the redundant altimeter. These are the altitudes that were used in both VDF/PDFs. There are three reasons why this change was made. The first reason is that this is the first year the team has used the SkyAngle Cert-3 XXL main parachute, and there was little previous data on the amount of vertical distance the parachute needed to fully open. Therefore, the altitudes were moved higher in an abundance of caution and because there is no minimum drift requirement for the vehicle demonstration flights. Via this method, the altitudes could be inconsequentially adjusted for the next flight if the amount of drift proved too high, which was the second reason for the change. The third reason the change was made (specifically why the redundant altimeter is set to deploy the main parachute 200' below the primary altimeter rather than 100') was because the first round of vacuum chamber testing suggested that the RRC3+ Sport altimeter has a tendency to deploy the main parachute at an altitude slightly higher than what it is set to. Therefore, the two signals were spaced out more to avoid possible simultaneous ignition.

The other significant change that has been made to the avionics and recovery system is that the primary and redundant altimeters have been switched around (the RRC3+ Sport altimeter is now the primary and the Telemetrum altimeter is now the redundant). Unlike the previous change, this change was made solely for the VDF/PDF #2. In the first flight, the ballistic impact caused significant damage to the team's Telemetrum v2.0 altimeter, so a new one was purchased for the second flight. Since the team's purchase of the first Telemetrum, there had been an upgrade to v3.0, which is what the team received after VDF/PDF #1. The vacuum chamber testing was run again with the new Telemetrum. However, slight software changes in how apogee is detected between the two versions of the Telemetrum caused anomalous results when the team's vacuum chamber test setup was used. The drogue parachute in these simulated flights was consistently deploying only a few hundred feet above the main parachute. So, in a further abundance of caution, the Telemetrum was relegated to being the redundant altimeter for the second flight. Fortunately, it did appear to perform nominally during the flight (see Figure 1.4 above), but the team will continue to use this configuration because it has been proven to be capable of producing a successful flight.

---

### **1.5.2. Changes Made to the Payload Design**

No changes were made to the design of the payload system since the initial Flight Readiness Review.

---

## 2. Results of Vehicle Demonstration Re-Flight

This section summarizes the re-flight of the full-scale rocket and discusses any successes and failures. The payload was included for both VDFs, so see Section 3 for an in-depth look into the results of the second payload demonstration flight and a comparison to the results of the first demonstration flight.

### 2.1. Summary of Vehicle Demonstration Flights

The vehicle was launched on March 7th, 2020 on a 4 grain CTI L1500 motor. The vehicle reached an altitude of approximately 4613ft (average). At apogee, the lower airframe and the rest of the launch vehicle successfully separated and released the drogue parachute. At 1000ft, the primary ejection charge ignited separating the upper airframe and the avionics bay; near approximately 700ft, the main parachute successfully deployed. There was an estimated 700ft of drift from the landing site, and the launch pad. More information on the payload demonstration can be found in Section 3.

### 2.2. Re-Flight Systems With Proper Functionality

All major systems functioned properly during the reflight.

- Drogue parachute deployed at apogee and the connections between the lower airframe and the rest of the launch vehicle remained completely intact.
- The main parachute deployed successfully, only slightly below the target deployment altitude of 1000ft.
- Retention and deployment functions of the launch vehicle behaved as expected, and restricted movement of the payload.
- All avionics components but GPS functioned properly and collected data for the entire duration of the flight.

### 2.3. Re-Flight Systems Without Proper Functionality

Unfortunately, the GPS on the Telemetrum altimeter did not log any data in this flight. This is because the Automatic Packet Reporting System (APRS) Interval was accidentally set to 0 rather than 5, preventing any GPS location data from being reported back and logged. Therefore, drift distance was estimated using the onboard video from the secondary payload camera system instead.

## 2.4. Flight Profile

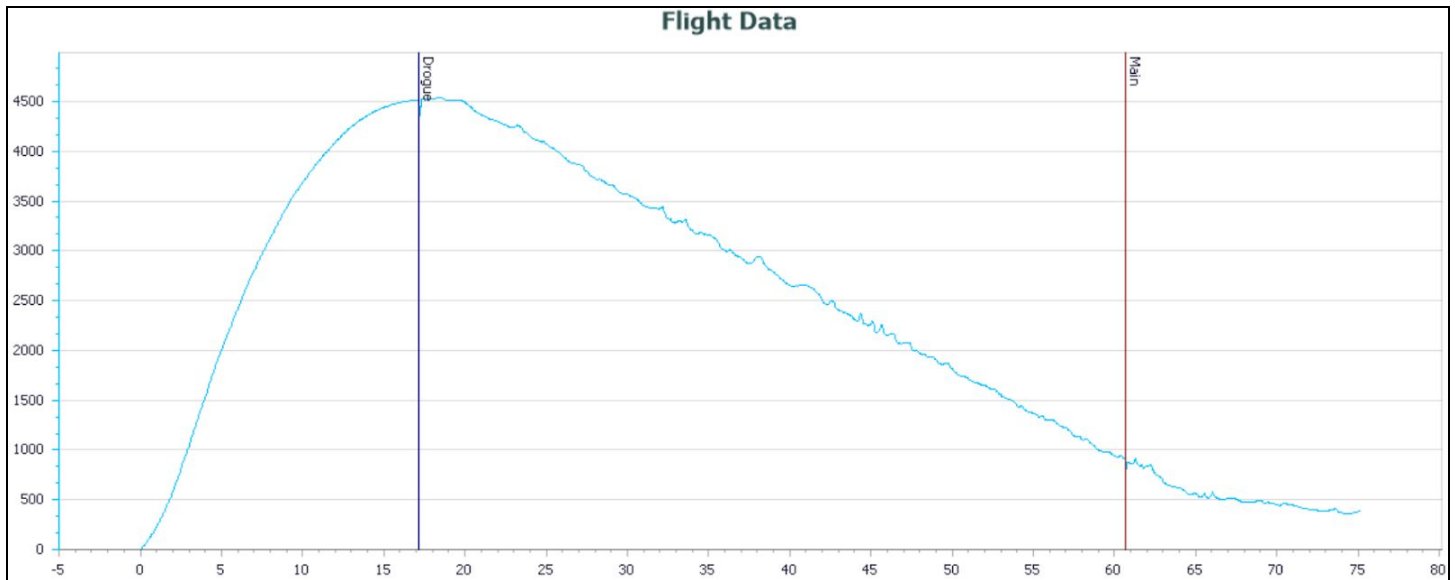


Figure 2.1: RRC3+ Sport Altimeter (Primary) VDF/PDF #2 Flight Profile

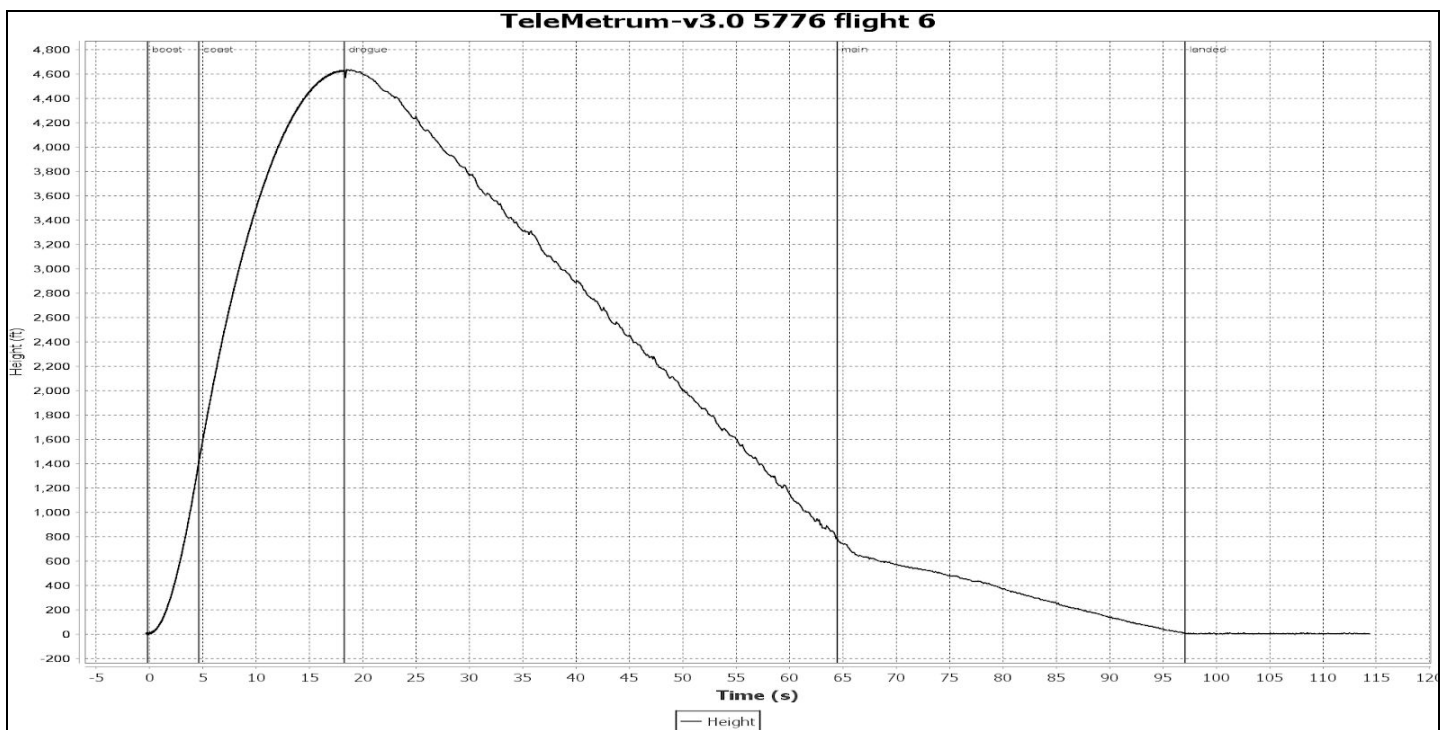


Figure 2.2: Telemetrum Altimeter (Redundant) VDF/PDF #2 Flight Profile

## 2.5. Updated Simulations

On the day of launch, the forecast showed wind speeds of about 9mph. Based on that, the team used 9mph wind speeds to run the launch day simulations. The results shown below were run

using the most up-to-date OpenRocket model, which weighs 55.5lbm, with a 3.5lbm ballast weight attached on the launch vehicle. Shown below are the resulting altitudes for each simulation run.

PSP-SL Ballasted Launch Vehicle Pre-Launch Simulations	
0 Inc, 9mph	4804'
5 Inc, 9mph	4652'
10 Inc, 9mph	4428'
15 Inc, 9mph	4125'

Table 2.1. Ballasted Launch Vehicle Pre-Launch Altitude Predictions

To estimate the drag coefficient, at first the most likely scenario, at 0 deg inclination and 9mph wind, was plotted in OpenRocket, with flight configuration, as described. The OpenRocket plot with Altitude, Total Velocity and Drag Coefficient vs Time can be seen in figure # below:

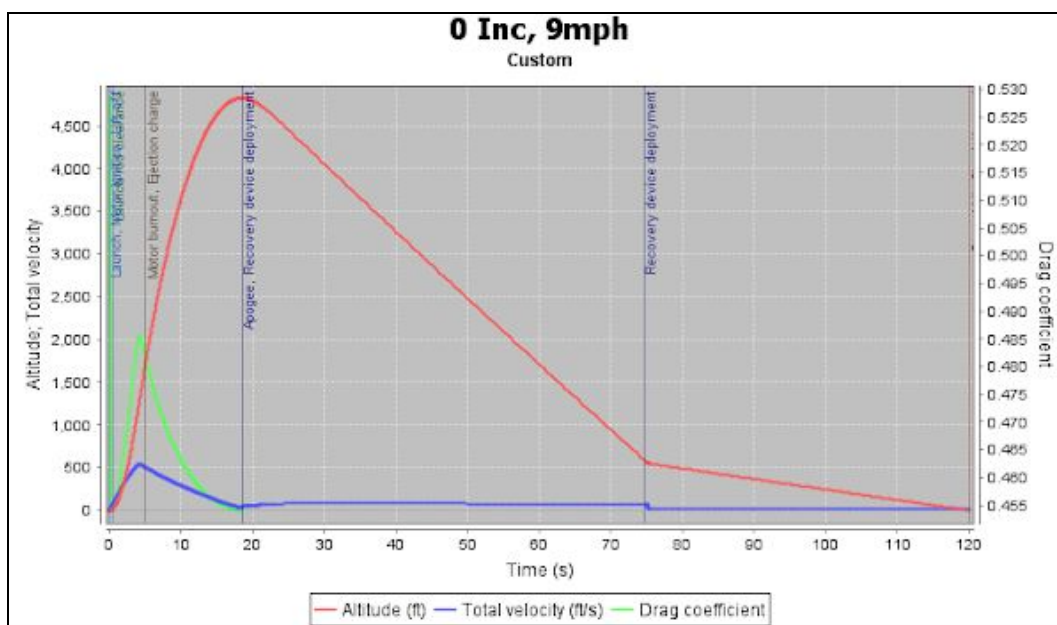


Figure 2.3: OpenRocket Altitude, Total Velocity and Drag Coefficient vs Time plot.

	Real Flight (RCC3+/Telemetry)	OpenRocket Simulation
Apogee (ft)	4601/ 4625	4804
Maximum Velocity (ft/s)	498 / 501	535

Table 2.2: Real data Vs OpenRocket simulation data

The predicted apogee from OpenRocket (') is not very close to the average altitude measured from the two altimeters (4613'). There is a deviation that is within 200ft of the average measured altitude. The maximum predicted velocity by open rocket deviates by a small amount from the RCC3+ Sport

data and from the Telemetry data, which both provide lower velocities than the simulation, within 40ft/s of the predicted velocity. The reason for the deviation is that OpenRocket assumes ideal (laminar) flow conditions, as well as translational movement of the launch vehicle only, excluding rotational movement.

As can be seen in the plot, the estimated maximum drag coefficient from the OpenRocket simulation is  $Cd(\max) = 0.53$ . Hand calculations were performed for the boost time interval from 0 to 4.48s. First, Telemetry data (specifically, the denser sampling rate) was used to find an equation for velocity. Excel was then used to find a trendline for velocity vs time. Using the momentum principle, the drag coefficient was then derived:

$$\Delta p = \int_0^{4.48} F_{net}(t)dt \Rightarrow p_f - p_i = \int_0^{4.48} F_{net}(t)dt \Rightarrow m_f * v_f = \int_0^{4.48} F_{net}(t)dt \text{ (Eqn. I)}$$



Figure 2.4: Free body diagram of Launch Vehicle during ascent.

From the free body diagram of the launch vehicle above,  $F_{net} = F_{motor} - F_{drag} - Weight$  (Eqn. II), assuming that all forces are vertical and that changes in weight and initial momentum are 0. From equations (I) and (II):

$$\begin{aligned} m_f * v_f &= \int_0^{4.48} [F_{motor}(t) - F_{drag}(t) - Weight(t)]dt \Rightarrow m_f * v_f \\ \Rightarrow m_f * v_f &= \int_0^{4.48} F_{motor}(t)dt - \int_0^{4.48} F_{drag}(t)dt - \int_0^{4.48} Weight(t)dt \\ \Rightarrow m_f * v_f &= \int_0^{4.48} F_{motor}(t)dt - \int_0^{4.48} [1/2 * \rho * v^2(t) * A * Cd]dt - \int_0^{4.48} [g * m(t)]dt \\ \Rightarrow m_f * v_f &= \int_0^{4.48} F_{motor}(t)dt - 1/2 * \rho * A * Cd * \int_0^{4.48} [v^2(t)]dt - g * \int_0^{4.48} [m(t)]dt \end{aligned}$$

Then, the equation was rearranged to get the Cd:

$$\Rightarrow Cd = [2 / (\rho * A * \int_0^{4.48} [v^2(t)]dt)] * [\int_0^{4.48} F_{motor}(t)dt - m_f * v_f - g * \int_0^{4.48} [m(t)]dt]$$

Then, the term  $v(t)$  was replaced with a second-order trendline from Excel:

$$v(t) = -3.1459 * t^2 + 48.836 * t + 2.4506 \text{ m/s (with } R^2 = 0.9991)$$

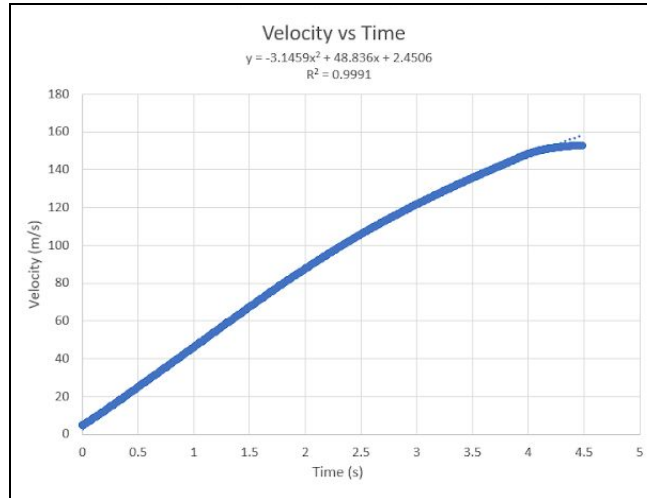


Figure 2.5: Telemetry Altimeter (Redundant) Velocity vs Time Plot.

The term  $m(t)$  is replaced with the third-order polynomial trendline from Excel:

$$m(t) = 0.0139 * t^3 - 0.042 * t^2 - 0.6334 * t + 25.195 \text{ kg (with } R^2 = 0.9991)$$

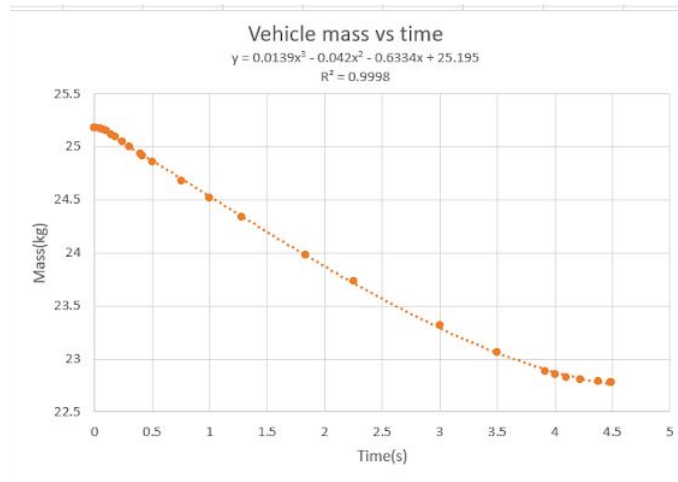


Figure 2.6: Mass vs Time Plot using data from ThrustCurve.org.

The integral  $\int_0^{4.48} F_{motor}(t)dt$  gave the motor's impulse, which is 5015 Ns. Then, a python script was used to calculate  $Cd = 0.77$ . Finally, this value is averaged with the OpenRocket simulation, to give  $Cd = 0.65$ . This value is more reasonable and could explain the smaller maximum velocity compared to the OpenRocket simulation.

A simulation was run to verify these results using a Vpython script on GlowScript IDE, with an estimated  $Cd$  of 0.65. This script used the momentum principle to update momentum via a loop:

$pf = pi + Fnet * \Delta t$ , with  $\Delta t = 0.001s$ . For the motor burn phase, thrust curve data was also used (from ThrustCurve.org) to create a trendline on Excel for the motor force, which was:

$F_{motor}(t) = -39.632 * t^6 + 580.31 * t^5 - 3304.3 * t^4 + 9114.9 * t^3 - 12322 * t^2 + 7021.5 * t + 376.54 N$  (with  $R^2 = 0.8692$ ). The trendline generated an integral that was very close to the motor impulse, 5021.8Ns. Next, after 4.48s, the motor's force is removed from the calculation of Fnet and thus momentum update is dependent on Fdrag and Weight alone. The results can be seen in Figures 2.7 and 2.8:

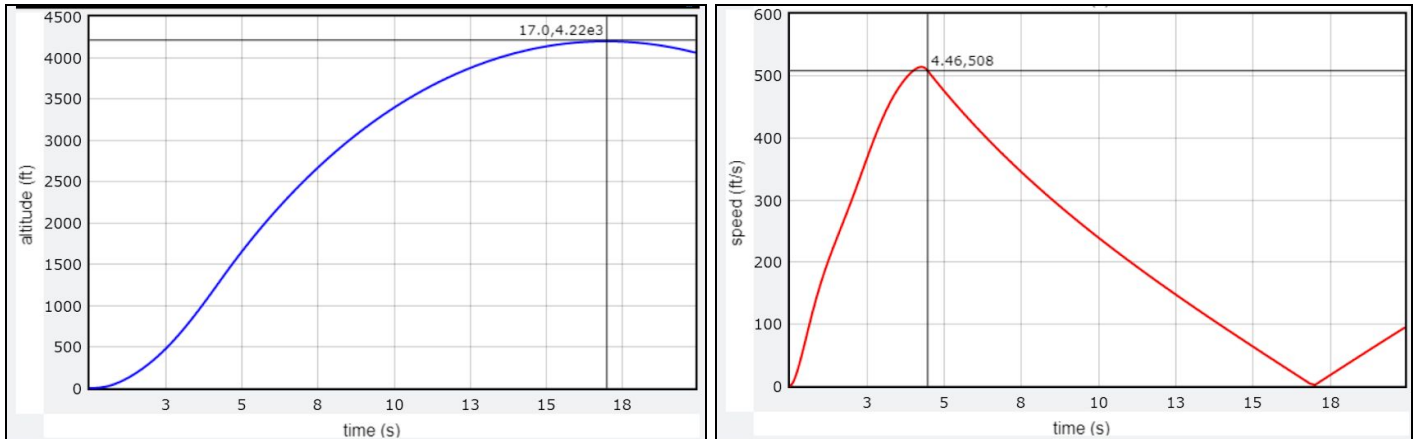


Figure 2.7: Altitude (ft) vs time (s) with VPython simulation (LEFT)  
 Figure 2.8: Velocity (ft/s) vs time (s) with VPython simulation (RIGHT)

From the altitude vs time and velocity vs time graphs, apogee occurs at approximately 4220ft at 17.0s, which is a relatively large deviation from the Telemetry data (within 400ft). The velocity at 4.46s is 508ft/s, with  $v_{max} = 515ft/s$ , which is close to the Telemetry data. The inaccuracies, especially in the simulated altitude, are mostly due to approximations in the thrust curve and in the calculations that were done to obtain the Cd.

## 2.6. Hardware Rebuilt Since VDF 1

- Identify any hardware that was damaged and required repair or replacement and discuss the plan of action.

### Avionics and Recovery

Following the first Vehicle Demonstration Flight, much of the avionics bay was replaced or rebuilt. The coupler, switch band, threaded rods, switches, and all 3D printed parts (avionics sled, battery guard, and switch holders) were replaced with identical parts due to extensive damage from the ballistic impact. The Telemetry altimeter (v2.0b) was also badly damaged on impact, so a new one was purchased (v3.0) to use for the second Vehicle Demonstration Flight as well as for all future flights. The Telemetry v2.0b is currently being repaired by Altus Metrum and will be available as a backup upon return. The terminal blocks on the RRC3+ Sport were replaced with new ones because incorrect handling (unrelated to the flight) caused the screws to become severely stripped. Finally, because the drogue shock cord, nomex blanket, and drogue parachute (24" Fruity Chutes Classic Elliptical) were lost with the lower airframe, they were also replaced with identical parts.

## Vehicle

During the first Vehicle Demonstration Flight, the lower airframe and all its components were lost. The launch vehicle flew through a cloud layer that was much lower than reported, and the team lost visual contact with it. The team heard the ejection charge that deployed the main recovery system, but when the launch vehicle came down, it was without the entire lower airframe. The team concluded that the quick link connecting the lower airframe assembly to the upper airframe must not have been properly connected. In the three weeks following the first Vehicle Demonstration Flight, the team worked to order parts and rebuild the lower airframe completely.

## 2.7. Lessons Learned Concerning the Vehicle

### Avionics and Recovery

One critical lesson learned from the first Vehicle Demonstration Flight is that it is important for each major section of the launch vehicle separated by shock cord (upper airframe, avionics bay, and lower airframe) to contain a GPS tracker. This need became apparent when the lower airframe completely separated from the rest of the launch vehicle and could not be found until after the second flight, as no location data for that specific section was available. Therefore, the team purchased two EggTimer transmitter/receivers, one to place in the upper airframe and one to place in the lower airframe, so location data for every section of the vehicle can be monitored during a flight. Because the avionics bay already contains a Telemetry (with GPS capability), an additional tracker is not required for this section. These transmitter/receivers did not arrive in time to be used in the second Vehicle Demonstration Flight, but the team is planning to utilize them in the final flight on Launch Day.

In addition, there was a considerable increase in the quality of team safety checklists for launch procedures which resulted from the first VDF/PDF's failure. These changes are explained in greater depth in Section 4.

Another critical lesson the team took away from the first Vehicle Demonstration Flight was the importance of double-checking procedures. The loss of the lower airframe was caused by a quick link being improperly connected. Had a member of the team checked the quick link's connection, this could have been avoided. From now on, the team will use detailed checklists for each subteam's launch preparation procedures and will have a member from a different subteam check the team's work to make sure it is properly done.

### Vehicle

The critical lesson the team learned was to double-check everything, from the securing of the quicklinks to the installment of the payload into the launch vehicle. The team developed thorough checklists, covering pre-launch procedures, as well as launch field procedures. Not only are the checklists to be checked by a member of the according subteam, but it is to be double-checked by a member of another subteam to ensure no small details are overlooked. By doing so, the team will be able to eliminate human-caused errors.

## 3. Results of Payload Demonstration Flights

This section summarizes the second attempt at completing the payload mission and effectively utilizing the payload retention and deployment (R&D) system and discusses any successes and failures.

### 3.1. Payload R&D System Design

Due to the nature of the events of the first PDF, in which all payload systems worked as intended up until the in-flight launch vehicle anomaly, no changes were made to the payload R&D system. Additional testing was done on the system in the time leading up to the second PDF attempt to ensure it would perform as intended during and after the flight. A summary of the R&D system design follows in Section 3.1.1.

#### 3.1.1. R&D Design Summary

The R&D system is comprised of four main sub-systems, each of which will be briefly described below.

##### 3.1.1.1. UAV Retention System

The UAV retention system is designed to safely retain the UAV during launch vehicle flight and during axial deployment then subsequent orientation. The UAV retention system, seen in Figure 3.1 below, uses a set of servo-controlled rack and pinion linear actuators to control the release of the airframe's passive X-Wing mechanism, to prevent any undesired vertical motion of the UAV, and to isolate power from the FCC while the UAV is inside the launch vehicle.

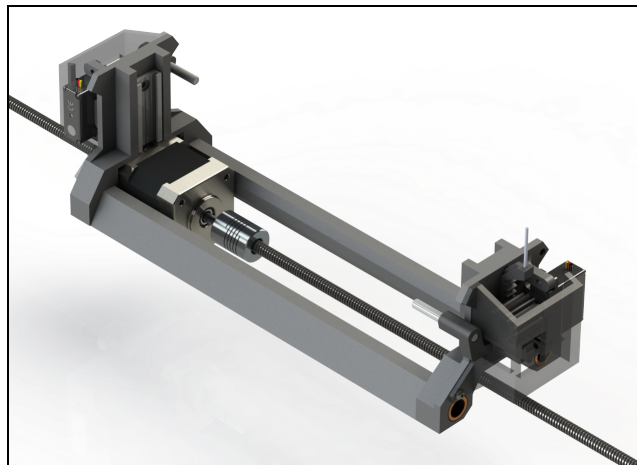


Figure 3.1: UAV Retention System

##### 3.1.1.2. Locking System

The system undergoes significant vibrational loads throughout the flight, as well as a significant deceleration during main parachute deployment. The R&D locking system is designed to firmly secure the launch vehicle's nosecone to the upper-airframe and keep the R&D system from expanding despite these forces.

The final locking system design makes use of the already present linear motion rods and orientation servo. Notches cut in the linear motion rods provide a detent that is interlocked with the forward and aft locking bulkhead before flight. This interlocking provides a robust load path between the upper airframe and nose cone. Note in Figure 3.2 that the load path completely bypasses the entire Axial Expansion and UAV Orientation system. This allows those systems to be designed solely kinematically, with little regard to intense flight loads.

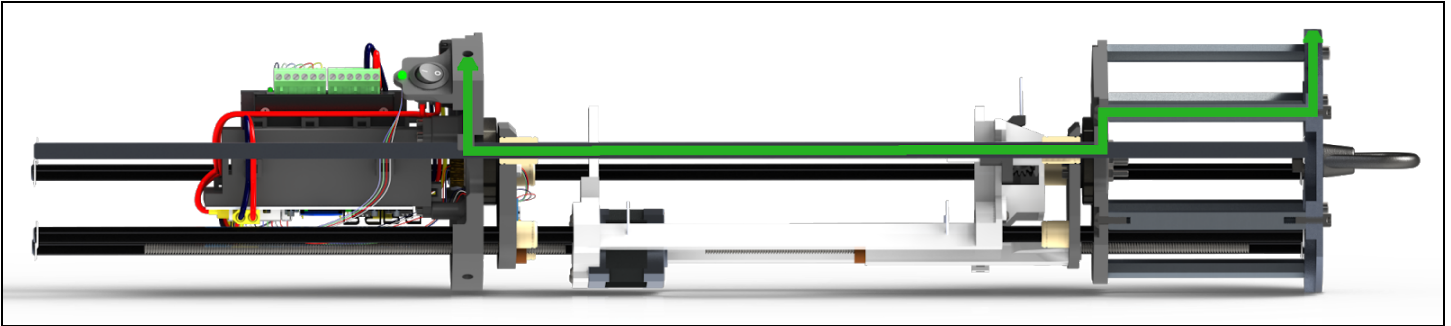


Figure 3.2: R&D section view showing a load path from the nose cone to the upper airframe (green)

While the notch detent system provides a load path for any axial flight loads, it would remain susceptible to vibration or off axis loads without a system preventing the rotation of rods and by extension, the unlocking of the detent notches. This is accomplished using the orientation servo motor and drive system. It is well known that a worm gear drive can only be driven in one direction. Using this fact and properly aligned gears that reduce movement between gear teeth without engagement (backlash), it becomes impossible for the system to be rotated (and by extension unlocked) without the activation of the orientation servo motor. The entire locking system was tested under a tension of 300lbs without failure, ensuring a factor of safety of 2 across the system.

After landing, the orientation servo motor and drive system are used to rotate the system into a state in which neither the linear motion rods or their corresponding retaining rings collide with the locking bulkheads. This state is confirmed with a limit switch attached to the forward locking bulkhead making contact with the Axial Expansion leadscrew. Once the system is in this state it is considered unlocked, and the UAV deployment process continues.

#### 3.1.1.3. Axial Expansion System

After safe landing and unlocking, the Axial Expansion System provides the UAV a clear flight path by moving both the UAV Sled and the nosecone relative to the upper airframe. The linear motion is controlled by 4 aluminum linear motion rods, and is powered with a dual shaft stepper motor and 2 lead screws. The 4 linear motion rods sit in a series of linear bearings which allow them to slide freely, only constrained by end mounted push-on retaining rings. These rings prevent asymmetrical loads in the system from causing the rods to disengage from one pivot plate before the other. Two of the linear motion rods also pass through the UAV Retention Sled, providing it support and alignment.

The UAV Retention Sled houses the dual shaft NEMA 17 stepper motor, which is attached via flexible couplings to right handed and left handed lead screws fore and aft respectively, shown in Figure 3.3. When the system is ready for expansion, the electronics bay commands the stepper to run for a predetermined number of steps, resulting in a precise expansion of 16 inches. The

handedness of the lead screws ensures that the UAV Retention Sled remains centered between the nose cone and upper airframe throughout this process. The Axial Expansion System has the effect of clearing the linear motion rods from the forward and aft locking plates, allowing the UAV Orientation Control System to function.

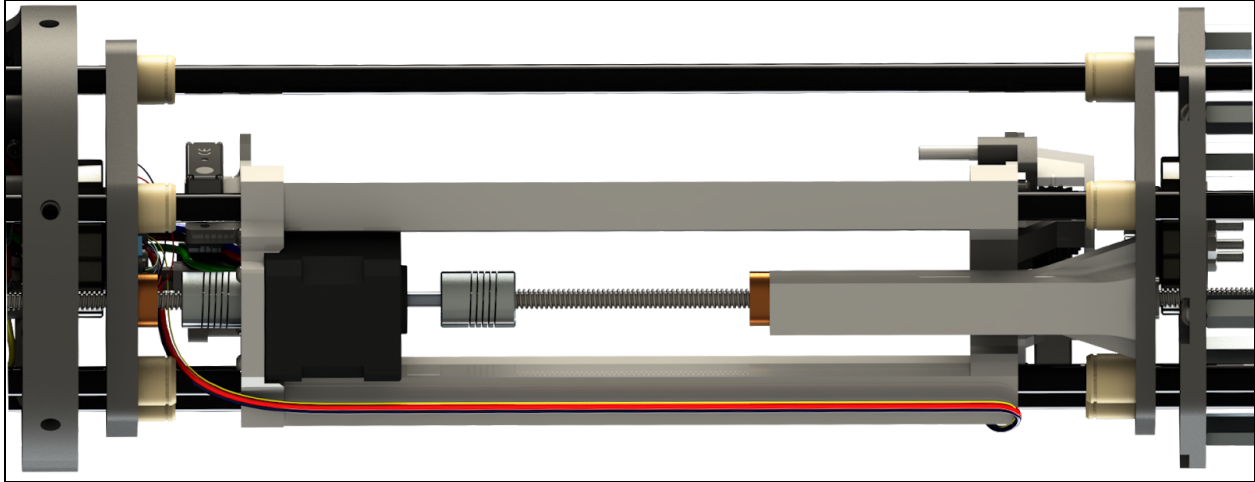


Figure 3.3: Underside of R&D System (UAV not shown)

#### 3.1.1.4. UAV Orientation Control System

Due to the chaotic nature of rocket recovery, the post-flight axial orientation of the upper airframe and by extension the UAV is unknown. The UAV Orientation Control System acts to align the UAV's vertical direction with gravity, such that it can take off vertically without interference from the ground or the rest of the R&D System.

The motion is controlled through a closed loop system consisting of a 6 axis accelerometer and a continuous rotation servo motor. Using data from the accelerometer, the orientation servo rotates a worm drive which slowly tilts the bay to the UAV launch orientation. The worm drive gives the system additional precision, and prevents any risk of backdrive.

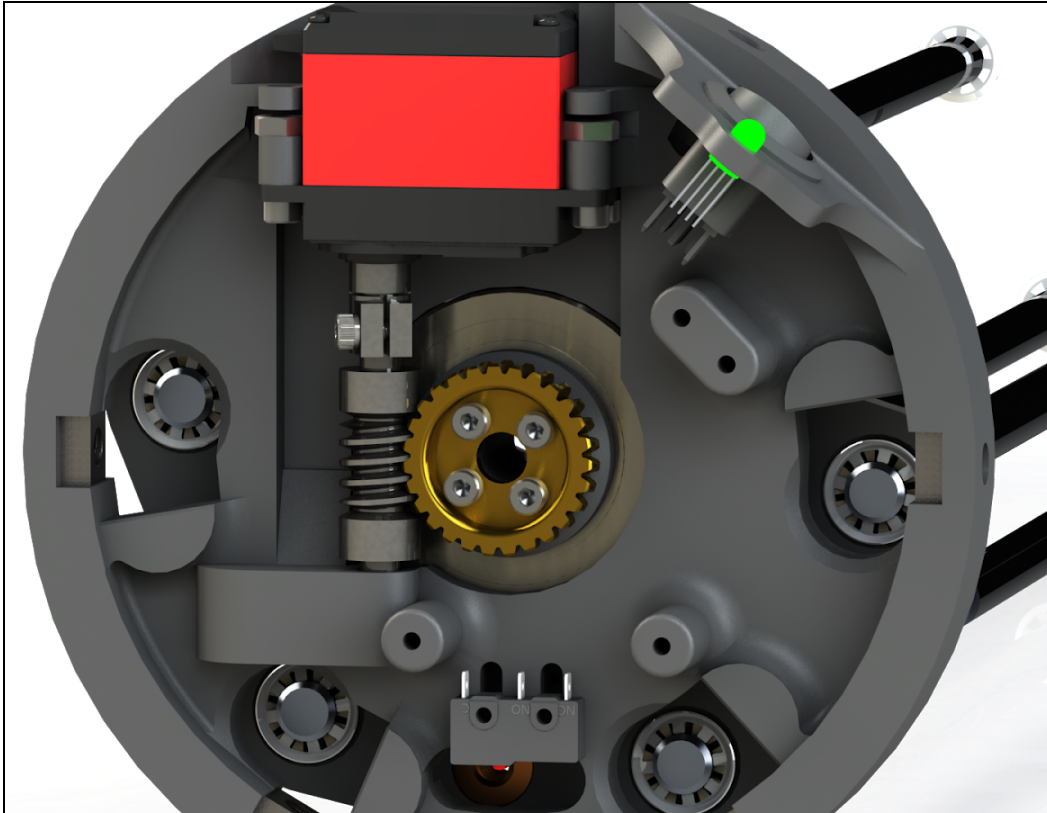


Figure 3.4: Forward R&D Subsystem (Electronics Bay not shown)

### 3.1.2. R&D Re-Flight Systems with Proper Functionality

The table below outlines the performance of all R&D sub-systems during and after the flight. As seen in the table, all systems performed as designed throughout the flight, and with the exception of one UAV deployment miscue, all systems also performed as designed during the deployment phase of the payload mission.

R&D Sub-System Performance		
Sub-System	Functionality	Success/Failure
UAV Retention System	Active Retention	Success
	Deployment	Failure
R&D Locking System	Locking In-Flight	Success
	Unlocking Post-Flight	Success
Axial Expansion	Full System Expansion	Success
Orientation Control System	UAV Orientation Control	Success
RF Communication	Wireless Communication/Command	Success

Table 3.1: R&D Sub-System Performance Overview

### 3.1.3. R&D Re-Flight Systems Without Proper Functionality

As seen above in Table 3.1, the deployment functionality of UAV Retention System was the sole system that did not perform with proper functionality during the mission. After the UAV was oriented to a roll angle of 0 degrees, the system’s servo motors were remotely triggered to actuate, allowing the UAV’s X-Wing mechanism to unfold into its flight configuration. When this was triggered, one X-Wing did not fully unfold, due to an error in the assembly of this sub-system prior to the flight. As a result, the X-Wing had to be unfolded by hand prior to the continuation of the payload mission. Due to the fact that this error occurred after the flight of the launch vehicle was successfully completed, this error was not deemed critical to the safety of the overall mission.

### 3.1.4. R&D Hardware Rebuilt Since PDF 1

All R&D hardware, with the exception of the aft-bulkplate, needed to be rebuilt and/or replaced after the first PDF. This included the R&D electronics package, the linear rods, the UAV sled, the entirety of the UAV orientation system, and many other miscellaneous R&D components. Despite the challenge imposed by this situation, the R&D system was completely rebuilt within one week of the first demonstration flight.

### 3.1.5. Lessons Learned Concerning R&D

Even with an extensive ground-testing campaign, the data provided by a demonstration flight will always yield new insight into the system. The Payload Team learned several lessons from this flight concerning R&D.

The primary takeaway from the flight was that the R&D system is more than capable of withstanding in-flight forces. The system kept the upper part of the launch vehicle together and kept the UAV secured to the sled throughout the entirety of the flight. A thorough inspection of all payload components after the flight showed no structural or superficial damage to any parts of the system.

This was true even with substantial winds at altitude that caused the upper part of the rocket to make contact with the lower-airframe numerous times during descent.

An additional takeaway from the flight was the need for better assembly instructions and methodology for the UAV retention system. The UAV retention system worked as intended during the flight, but failed to fully unlock the UAV for deployment after the launch vehicle successfully landed. This failure was due to an assembly error when preparing the rack-and-pinion assembly on the R&D sled prior to the flight. After the flight, a full investigation was conducted into how this error could be mitigated in the future. This investigation concluded that a set of thorough steps on the installation of the vertical gear assembly was necessary so that all payload personnel could assemble the system in the future.

## **3.2. Payload Mission**

### **3.2.1. Payload Mission Design Summary**

There were a few differences from PDF mission sequence as opposed to the final mission design that will fly in April. Most notably, this mission sequence called for manual operation of the UAV as opposed to the designed semi-autonomous flight functionality. This was due to delays in the software development of this system. An additional alteration to the final projected mission sequence was the way in which the ice mining and procurement system (IMPS) was triggered. Due to delays in software development, the IMPS needed to be triggered by hand, using a rocker switch installed on the UAV. Finally, the Ground Control Station (GCS) used during this flight was a much more primitive form of the final design that will be used later. This consisted of two laptops running early versions of the GCS software. This was also due to delays in software development. Figure 3.5 below outlines the payload mission design for the second attempted PDF. Note that the red blocks in the figure refer to the contingencies outlined in Table 3.2 below.

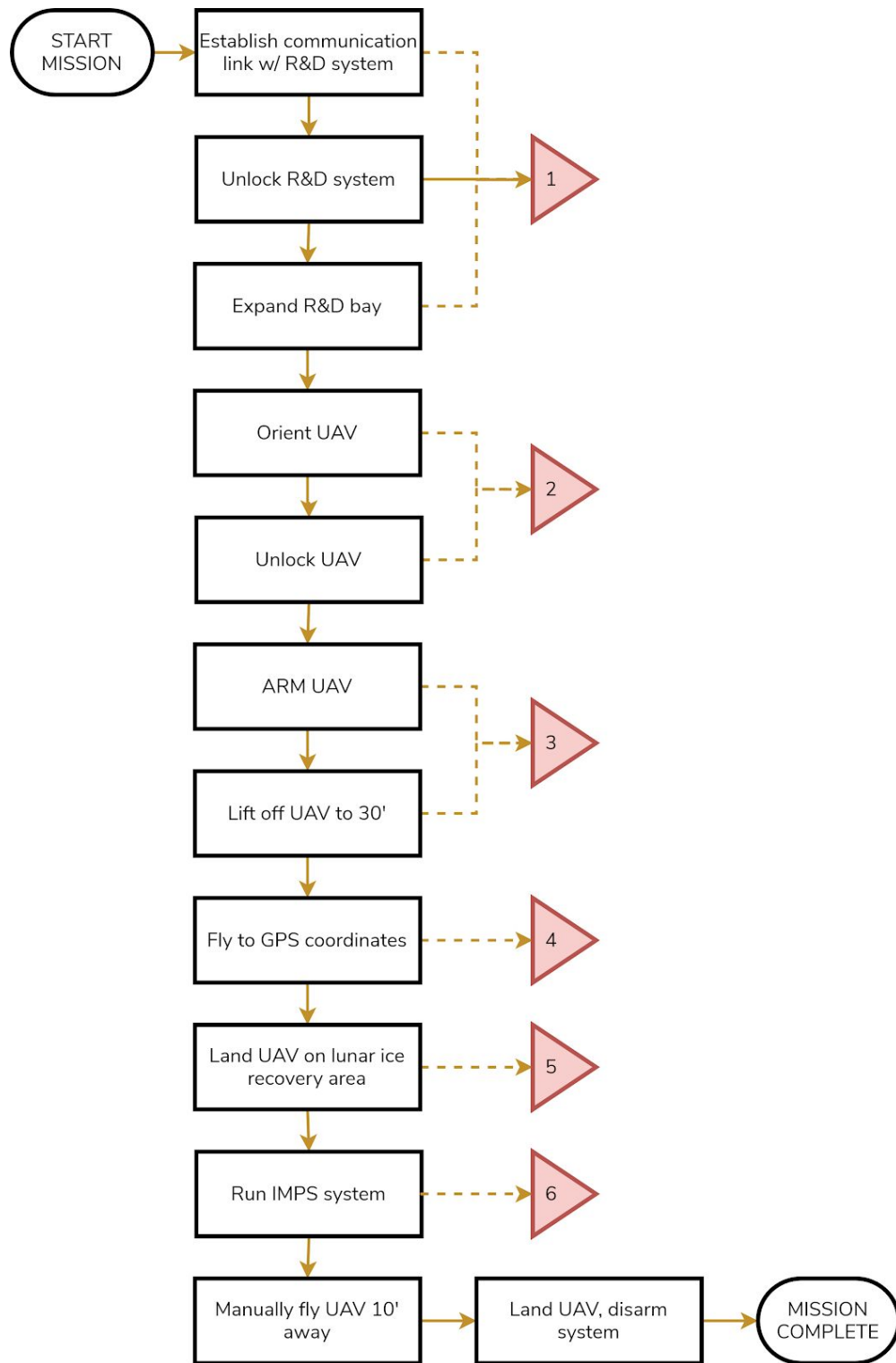


Figure 3.5: PDF Mission Sequence

Payload Mission Contingencies		
No.	Description	Action
1	R&D bay will not open	Manually separate upper-airframe from the nose cone. Proceed to contingency 2.
2	Unable to release UAV	Manually release UAV from R&D system. Place UAV on unlocked sled. Proceed through the rest of the mission.
3	UAV unable to lift off	Place UAV on level surface next to rocket. Proceed through the rest of the mission.
4	GPS navigation error	Manually fly UAV with RC transmitter to ice mining recovery area.
5	Recovery area landing failure	Disarm the UAV. Manually place the UAV on the lunar ice recovery area. Proceed through the rest of the mission.
6	Ice mining system failure	Inspect all bullet connections. If no visible issues, restart the Raspberry Pi. Wait 90 seconds for the Pi to boot up. Try running the ice mining motors again.
7	UAV battery low	If before UAV lifts off, note mission time and replace battery. Otherwise, abort mission.
8	UAV flight anomaly	Consult safety team. Remove LiPo (if safe). Recover UAV and abort mission.
9	Launch vehicle anomaly	Consult safety team. Attempt to recover payload system. Abort mission.
10	GCS failure	Restart GCS software and try again. If unsuccessful, attempt to run in XCTU. If still unsuccessful, attempt on a secondary computer.

Table 3.2: Payload Demonstration Flight Contingencies

### 3.2.2. Payload Re-Flight Systems With Proper Functionality

Table 3.3 below outlines the performance of the payload system during and after the PDF. Refer to Table 3.1 above for details of the performance of the R&D system during the flight.

Payload Sub-System Performance		
Sub-System	Functionality	Success/Failure
UAV	Deployment from sled	Failure

	Flight to lunar ice site	Failure
	Autonomous flight/landing	Not Attempted
IMPS	Actuation	Success
	Ice retention (>10 mL)	Success
GCS	Bi-directional communication	Success
	UAV command and control	Not Attempted
	R&D command and control	Success

Table 3.3: Payload Subsystem Performance Overview

As seen in the table above, the IMPS and GCS systems worked as intended, within scope of the designed mission profile for the PDF. The IMPS utilized only one of its two scoops on this flight, but still collected 12 mL of simulated lunar ice. This was deemed a major success, as the final iteration of the system will employ a second identical scoop, adding to the total amount of lunar ice material the payload can collect. As noted above, the GCS had limited scope in the PDF mission design due to developmental delays, but the functionality that was tested during this flight worked successfully. The GCS was able to communicate with the payload system prior to the launch, while the launch vehicle sat on the pad, as well as after the flight during the payload deployment phase of the mission. All deployment commands were successfully transmitted wirelessly to the payload, initiating each step of the deployment sequence. In addition, all data packets sent from the payload back to the GCS were received successfully.

### 3.2.3. Payload Re-Flight Systems Without Proper Functionality

As seen in Table 3.3 above, the primary system that did not perform as intended was the UAV. Upon successful expansion and orientation of the payload, the first failure occurred when the UAV was unlocked from the UAV retention system. When this system was activated, only one of the two armatures of the X-Wing mechanism unfolded into its flight configuration. Additionally, the pin triggering the UAV to initiate its startup sequence did not fully disengage from the limit switch. This meant that the UAV did not boot up as intended. Following the payload team's contingency plan, the UAV's X-Wing mechanism was manually unfolded and the UAV was turned on by hand. This failure was a result of incorrect assembly of the UAV retention system and has since been tested to ensure the failure is mitigated in the future.

The second failure occurred when the UAV was manually lifted off from its position on the R&D sled. Approximately three seconds into the lift-off sequence, a propeller nut securing one of the UAV's four propellers came loose and was ejected from the vehicle. This in turn caused the propeller to be ejected as well. Following the payload contingency plan, the UAV was immediately disarmed. As the propeller nut could not be found, it was determined to scrub the flight of the UAV. This failure was caused by UAV assembly error. A thorough investigation of this failure concluded that the propeller nuts were not properly secured with adhesive as designed. This assembly failure was the result of

---

insufficient assembly procedures and checklists. This issue has since been rectified and the payload team is confident that such a failure will not occur in the future.

#### **3.2.4. Payload Hardware Rebuilt Since PDF 1**

All payload hardware, with the exception of the GCS, had to be rebuilt since the first attempted PDF. This included the entirety of the UAV airframe, all UAV electronics, the UAV propulsion system, and all aforementioned R&D components described in section 3.1.4.

#### **3.2.5. Lessons Learned Concerning the Payload**

In addition to the lessons learned concerning R&D outlined above in section 3.1.5, there was an additional lesson learned about the payload system overall. The payload team learned the need for consistent and thorough testing of all systems prior to launch. The R&D system was thoroughly ground tested in the weeks leading up to both demonstration flights. During this time, multiple minor tweaks and changes were made to the system to improve its consistency and overall performance. The R&D system in turn worked nearly completely as intended during the demonstration flight. Continuous development of the UAV in the days and weeks prior to the launch prevented such a thorough test campaign of this system. It should have come as no surprise then, when this system did not perform as intended during the launch. In the weeks since the PDF, such a test campaign has been initiated to ensure consistent performance of the UAV for the mission in April.

## 4. Changes Made to Team Safety since VDF/PDF #1

This section summarizes changes made to safety considerations as a result of the experiences made during the failed vehicle demonstration flight.

### 4.1. Checklist Improvements

The implementation of checklists made before the Flight Readiness Review revealed critical lapses in content: poor application of quality witness steps and a clear misunderstanding of flight procedures resulted in a lack-luster checklist that was largely left unused during the vehicle demonstration flight, resulting in general team confusion and a lack of launch procedure continuity. There was a good deal of confusion during the launch vehicle preparation stage, as well as excessive peripheral actions, including the flying of unrelated drones and other miscellaneous activities not related to launch vehicle operations, which largely served to obstruct the work space and add to the general confusion of the launch field.

Pursuant to improvement in these critically lacking areas, the safety team immediately pursued a more clear image of the ideal launch: discussion was had between the team safety officer and the other team leads. These discussions lead to the creation of in depth, goal-oriented, subteam-centric checklists designed to not only add to the overall launch day team cohesion, but also to help the subteams remember critical tasks and goals to be met to ensure successful completion of the launch vehicle.

The improved checklists lay out an organized list of all actions required to successfully build a fully integrated launch vehicle for the purposes of this competition. Each subteam has included their input for critical milestones of the process (which became checklist headings) and each step needed to complete the milestones.

### 4.2. Quality Witness Improvements

In general, the team found that the quality witness steps included in the checklist worked to the extend they were written. However, real-world experience demonstrated to the team not only that a more comprehensive list of quality witness steps would be beneficial, but also that the witnesses could serve another critical purpose: ensuring the over all completion of the launch vehicle.

The quality witness steps previously included in the team checklists worked well for the team's purposes, and in fact led many other team leads to request for more steps to cover more areas of the construction process. Due to the failures the team suffered at the first demonstration flight, however, it became clear that accountability was needed for the overall construction process; the team felt that quality witnesses filled that need. As a result, a restructuring of the quality witness process was done; a quality witness step was to follow the completion of every major step in the launch vehicle construction process (Payload UAV preparation, main parachute connection, lower airframe integration, etc). The "witnesses" would serve to confirm whether or not a critical step (as mentioned above) had been completed. Upon completion of the launch vehicle construction process, the safety officer will list the quality witness steps by name, and the witnesses will confirm their completion. If any witness cannot confirm the completion of their respective step, the step will be repeated, and all relevant quality witnesses will be redone. Witnesses will also sign off on the completion of their respective steps.

## 5. Official Altimeter Data

### 5.1. Initial Flight (VDF/PDF 1) on 2/15/2019

Missile Works RRC3+ Sport		Altus Metrum Telemetry	
Apogee (Height AGL) (ft)	4688.00	Apogee (Height AGL) (ft)	4488.00
Ascent Time (s)	17.70	Ascent Time (s)	17.50
Drogue Deployment Altitude (ft)	4712.13	Drogue Deployment Altitude (ft)	4364.07
Drogue Deployment Time (s)	17.70	Drogue Deployment Time (s)	17.28
Main Deployment Altitude (ft)	673.70	Main Deployment Altitude (ft)	1007.48
Main Deployment Time (s)	46.05	Main Deployment Time (s)	45.88
Drogue Descent Velocity (ft/s)	142.00	Drogue Descent Velocity (ft/s)	123.00
Main Descent Velocity (ft/s)	118.00	Main Descent Velocity (ft/s)	130.00
Descent Time (s)	38.45	Velocity off of Launch Rail (ft/s)	72.97
Total Flight Time (s)	56.15	Descent Time (s)	35.40
		Total Flight Time (s)	52.90
		Drift Displacement (ft)	512.00

Table 5.1: VDF/PDF #1 Official Data

### 5.2. Re-Flight (VDF/PDF 2) on 3/7/2019

Missile Works RRC3+ Sport		Altus Metrum Telemetry	
Apogee (Height AGL) (ft)	4601.00	Apogee (Height AGL) (ft)	4625.00
Ascent Time (s)	17.15	Ascent Time (s)	18.40
Drogue Deployment Altitude (ft)	4510.82	Drogue Deployment Altitude (ft)	4624.18
Drogue Deployment Time (s)	19.20	Drogue Deployment Time (s)	18.48
Main Deployment Altitude (ft)	740.15	Main Deployment Altitude (ft)	639.53
Main Deployment Time (s)	62.70	Main Deployment Time (s)	66.48
Drogue Descent Velocity (ft/s)	85.00	Drogue Descent Velocity (ft/s)	83.00
Main Descent Velocity (ft/s)	27.00	Main Descent Velocity (ft/s)	24.00
Descent Time (s)	58.05	Velocity off of Launch Rail (ft/s)	68.27
Total Flight Time (s)	75.20	Acceleration at Main Deployment (ft/s <sup>2</sup> )	86.88
		Descent Time (s)	78.80
		Total Flight Time (s)	97.30
		Drift Displacement (ft)	700.00 (estimated)

Table 5.2: VDF/PDF #2 Official Data